Chimeric anti-podoplanin antibody suppresses tumor metastasis through neutralization and antibody-dependent cellular cytotoxicity

Mika Kato Kaneko,[1,8] Akiko Kunita,[2,8] Shinji Abe,[3,8] Yuta Tsujimoto,[1,4,8] Masashi Fukayama,[2] Kaoru Goto,[4] Yoshihiko Sawa,[5] Yasuhiko Nishioka[6] and Yukinari Kato[1,7]

[1]Molecular Tumor Marker Research Team, Global COE Program, Yamagata University Faculty of Medicine, Yamagata; [2]Department of Pathology, Graduate School of Medicine, The University of Tokyo, Tokyo; [3]Practice Room for Clinical Pharmacy, Institute of Health Biosciences, The University of Tokushima Graduate School, Tokushima; [4]Department of Anatomy and Cell Biology, Yamagata University School of Medicine, Yamagata; [5]Department of Morphological Biology, Fukuoka Dental College, Fukuoka; [6]Department of Respiratory Medicine and Rheumatology, The University of Tokushima Graduate School, Tokushima, Japan

Podoplanin is a platelet aggregation-inducing factor associated with tumor metastasis, malignant progression, and cancer stem cells. We produced a rat–human chimeric anti-podoplanin mAb, NZ-8, from rat anti-podoplanin mAb (NZ-1). Although both NZ-1 and NZ-8 possess high binding affinities and high neutralizing activities of platelet aggregation, the antibody-dependent cellular cytotoxicity and complement-dependent cytotoxicity of NZ-8 were much higher than NZ-1. Furthermore, both NZ-1 and NZ-8 inhibited the growth of podoplanin-expressing tumors in vivo. Both NZ-1 and NZ-8 also suppressed hematogenous metastasis of podoplanin-expressing tumors. These results suggest that anti-podoplanin mAbs suppressed hematogenous metastasis by both neutralization and antibody-dependent cellular cytotoxicity/complement-dependent cytotoxicity activities. Targeting therapy to podoplanin-expressing tumors should be useful as a novel immunotherapy. (*Cancer Sci*, doi: 10.1111/j.1349-7006.2012.02385.x, 2012)

Podoplanin is a platelet aggregation-inducing factor, and its expression has been reported in many tumors including malignant brain tumors, mesotheliomas, and squamous cell carcinoma.[1–10] Importantly, recent investigations have suggested that expression of podoplanin is associated with tumor metastasis, malignant progression, and epithelial–mesenchymal transition.[11–18] Podoplanin expression has also been reported to be associated with clinical outcome.[19–21] Recently, we have shown podoplanin expression in atherosclerotic lesion.[22]

In solid tumors such as brain tumors, only a small and phenotypically distinct subset of cells could be responsible for generating and sustaining tumors, and thus be considered as cancer stem cells or tumor-initiating cells (TICs).[23] Because TICs are thought to be resistant to conventional therapies, and are responsible for relapse, targeting TICs could be a promising approach to cancer therapy.[24] Podoplanin has been reported to be a TIC marker;[25] therefore, immunotherapy using specific antibodies reactive to podoplanin may eradicate TICs in cancers.

We previously produced an anti-podoplanin antibody, NZ-1.[5] NZ-1 should have not only high specificity and sensitivity but also high binding-affinity against podoplanin to be applied for radioimmunotherapy or immunotoxin therapy. Previous studies showed that NZ-1 is a suitable candidate for therapy against malignant gliomas because NZ-1 was highly internalized into glioma cell lines, and also well accumulated into tumors *in vivo*.[26] Moreover, NZ-1 inhibited tumor cell-induced platelet aggregation and tumor metastasis by its neutralizing activity.[12] However, it has not been clarified whether

NZ-1 possesses antibody-dependent cellular cytotoxicity (ADCC) or complement-dependent cytotoxicity (CDC) against podoplanin-expressing tumor cells.

In this study, we produced rat–human chimeric anti-podoplanin antibody (NZ-8) from rat anti-podoplanin neutralizing antibody (NZ-1), and characterized NZ-8 activity in flow cytometry, Western blot, platelet aggregation, and ADCC/CDC analyses *in vitro*. Next, we investigated the antitumor and antimetastatic activities of the anti-podoplanin mAbs *in vivo*.

Materials and Methods

Cell lines and stable transfectants. Chinese hamster ovary, glycan-deficient CHO cell lines (Lec1, Lec2, and Lec8), and human malignant mesothelioma cell line H226 cells were obtained from ATCC (Manassas, VA, USA).[27] Human lymphatic endothelial cells were obtained from Cambrex (Walkersville, MD, USA). The CHO cells transfected with human podoplanin (CHO/hPDPN) were established as described previously.[1] Both CHO/hPDPN cells and H226 cells were cultured in RPMI-1640 medium (Wako Pure Chemical Industries, Osaka, Japan) supplemented with 10% heat-inactivated FBS (Life Technologies, Carlsbad, CA, USA), 2 mM L-glutamine (Life Technologies), 100 U/mL penicillin, 100 μg/mL streptomycin (Life Technologies), and 1 mg/mL geneticin (G418; Wako Pure Chemical Industries) for CHO/hPDPN at 37°C in a humidified atmosphere of 5% CO_2 and 95% air. The human glioblastoma cell lines LN319 and D397, donated by Dr. Webster K. Cavenee (Ludwig Institute for Cancer Research, San Diego, CA, USA) and Dr. Darell D. Bigner (Duke University Medical Center, Durham, NC, USA), respectively, were cultured in DMEM (Wako Pure Chemical Industries) supplemented with 10% heat-inactivated FBS, 2 mM L-glutamine, 100 U/mL penicillin, and 100 μg/mL streptomycin. Human lymphatic endothelial cells were cultured in endothelial cell medium EGM-2MV supplemented with 5% FBS (Cambrex).

Animals. Female BALB/c nude (nu/nu) mice (7 weeks old) were purchased from Charles River Japan (Kanagawa, Japan). Male Wistar rats, 6 weeks old, were obtained from CLEA Japan (Osaka, Japan). Animals were housed under pathogen-free conditions. The Animal Care and Use Committees of Yamagata University (Yamagata, Japan), the University of Tokyo (Tokyo, Japan), and the University of Tokushima (Tokushima, Japan) approved the animal experiments described herein.

[7]To whom correspondence should be addressed.
E-mail: yukinari-k@bea.hi-ho.ne.jp
[8]These authors contributed equally to this work.

Antibodies. A rat anti-human podoplanin mAb (IgG_{2a}), NZ-1, was developed as described previously.[5] Rat IgG and human IgG were purchased from Beckman Coulter (Fullerton, CA, USA). For the generation of rat–human chimera anti-human podoplanin (NZ-8), the appropriate V_H and V_L cDNAs of a rat NZ-1 antibody and C_H and C_L of human IgG_1 were subcloned into pcDNA3.3/Neo or pcDNA3.1/Zeo vectors (Life Technologies), respectively. Antibody expression vectors were transfected into CHO cells using Lipofectamine 2000 reagent (Life Technologies). Stable transfectants of CHO/NZ-8 were selected by cultivating the transfectants in medium containing 1 mg/mL geneticin and 0.5 mg/mL zeocin (Life Technologies).

Flow cytometry. LN319, D397, and H226 cells were harvested by brief exposure to 0.25% Trypsin/1 mM EDTA (Wako Pure Chemical Industries). After washing with PBS, the cells were treated with NZ-1 or NZ-8 (1 µg/mL) for 30 min at 4°C followed by treatment with Oregon green-conjugated anti-rat IgG or FITC-conjugated anti-human IgG (Life Technologies). Fluorescence data were collected using a FACSCalibur flow cytometer (BD Biosciences, Braintree, MA, USA).

Determination of binding-affinity by flow cytometry. Binding-affinity was determined as described previously.[28] Briefly, LN319 cells (2×10^5) were resuspended at 100 µL of serially diluted antibodies (0.01–20 µg/mL), followed by secondary antibodies (Life Technologies). Fluorescence data were collected using a FACSCalibur flow cytometer (BD Biosciences). The dissociation constants (K_D) were obtained by fitting the binding isotherms using the built-in one-site binding models in Prism software (GraphPad Software Inc., La Jolla, CA, USA).

Determination of binding-affinity by ELISA. The ELISA was carried out as described previously.[29] Briefly, the synthetic peptide EGGVAMPGAEDDVV (hpp3851), corresponding to amino acids 38–51 of human podoplanin was immobilized at 1 µg/mL. The plates were incubated with serially diluted antibodies (150 pg/mL–2.5 µg/mL), followed by 1:1000 diluted peroxidase-conjugated anti-mouse IgG (Dako, Glostrup, Denmark). The dissociation constants (K_D) were obtained by fitting the binding isotherms using the built-in one-site binding models in Prism software.

Western blot analyses. Cultured cell pellets were lysed with PBS with 1% TritonX-100 for 30 min on ice. Cell lysates containing 5 µg total protein were boiled in SDS sample buffer (50 mM Tris, 2% SDS, 5% glycerol, 10% 2-mercaptoethanol, pH 6.8). They were electrophoresed on 5–20% polyacrylamide gels (Wako Pure Chemical Industries), and were transferred to a PVDF membrane (Bio-Rad Laboratories, Philadelphia, PA, USA). After blocking with 4% skim milk in PBS, the membrane was incubated with NZ-1 or NZ-8 (1 µg/mL) then with peroxidase-conjugated secondary antibodies (1:1000 dilution; Dako) and developed with ECL-plus reagents (GE Healthcare, Buckinghamshire, UK) using Sayaka-Imager (DRC, Tokyo, Japan).

Preparation of effector cells. Rat splenocytes were harvested from Wistar rat spleens.[30] After depletion of red blood cells, splenocytes were used as effector cells. Human peripheral blood mononucuelar cells (MNC) were obtained from leukocytes, which were separated from peripheral blood of healthy donors as described previously.[31] The human study was approved by the ethics committee of the University of Tokushima, and written informed consent was obtained from all subjects.

Antibody-dependent cellular cytotoxicity (ADCC). The ADCC was evaluated using a ^{51}Cr release assay as described previously.[30] Target cells were targeted with 0.1 µCi of ^{51}Cr-sodium chromate at 37°C for 1 h. ^{51}Cr-labeled target cells were placed in 96-well plates in triplicate. Effector cells and antibodies (NZ-1, NZ-8, control rat IgG, control human IgG)

were added to the plates. After a 6-h incubation, 100 µL supernatant was measured in a gamma counter (PerkinElmer, Waltham, MA, USA). Percent of cytotoxicity was calculated from the following formula: %Specific lysis = $(E - S)/(M - S) \times 100$, where E is the release in the test sample, S is the spontaneous release, and M is the maximum release.

Complement-dependent cytotoxicity (CDC). The CDC was determined by ^{51}Cr release assay.[30] Target cells were incubated with 0.1 µCi of ^{51}Cr-sodium chromate at 37°C for 1 h. After incubation, the cells were washed three times with medium. ^{51}Cr-labeled cells were added into 96-well plates, and incubated with baby rabbit complement and NZ-1, NZ-8, control rat IgG, or control human IgG for 6 h. ^{51}Cr release of the supernatant from each well (100 µL) was measured using a gamma counter. Percent of cytotoxicity was calculated as above.

Antitumor activity of anti-podoplanin antibodies. CHO/hPDPN was suspended after trypsin treatment, washed with PBS, suspended in Hanks' balanced salt solution without calcium or magnesium, adjusted to a density of 3.0×10^7 cells/mL, and s.c. implanted into BALB/c nude mice at a dose of 100 µL/animal. NZ-1 or rat IgG was loaded in an Alzet mini-osmotic pump (model 2002; Durect, Cupertino, CA, USA), implanted into the peritoneal cavity of mice, and given at 2.5 µg/h for 2 weeks sustainably (NZ-1 experiments: control group, $n = 10$; NZ-1 group, $n = 9$). One hundred micrograms of NZ-8 or normal human IgG was given i.p. once a week, four times in total (NZ-8 experiments: $n = 10$/group).

Platelet aggregation assay. Platelet aggregation was monitored by measuring electric impedance using a whole-blood aggregometer Model 560 (Chrono-Log, Havertown, PA, USA).[9] Heparinized blood was drawn from BALB/c mice by cardiac puncture, and 500 µL whole blood was diluted with 500 µL normal saline. The specimen was placed in a plastic cuvette containing a magnetic stir bar, and incubated at 37°C for 10 min before testing. The platelet aggregation was then initiated by the addition of CHO/hPDPN (2×10^6 cells) and monitored for up to 20 min.

Experimental lung metastasis. CHO/hPDPN was harvested, washed, and resuspended in PBS (5×10^6 cells/mL). Next, the cells were incubated with NZ-1, NZ-8, or human IgG, and inoculated i.v. (5×10^5 cells/mouse) into the lateral tail vein of female BALB/c-nu/nu mice. After 19–20 days, the mice were killed, and the surface lung metastatic foci were counted and measured.

Statistical analysis. All data are shown as the mean ± SEM. Student's t-test, one-way ANOVA followed by Tukey–Kramer multiple comparisons, or two-way ANOVA were carried out, where appropriate. P-values <0.05 were considered statistically significant. All statistical tests were two-sided.

Results

Production and characterization of chimeric anti-podoplanin antibody (NZ-8). We first generated the rat–human chimeric antibody (NZ-8) by fusing the V_H and V_L regions of rat antibody (NZ-1) with C_H and C_L regions of human IgG_1, respectively. As depicted in Figure 1(A), NZ-8 reacted with both human glioblastoma cell lines LN319 and D397, and human mesothelioma cell line H226 in flow cytometry, although the NZ-8 reaction seems to be weaker than that of NZ-1. We previously produced several podoplanin-transfected glycan-deficient CHO cell lines, such as Lec1, Lec2, and Lec8, to investigate the involvement of O-glycan or N-glycan to podoplanin-induced platelet aggregation.[27] As shown in Figure 1(B), NZ-8 reacted with all podoplanin-transfected glycan-deficient CHO cell lines in the same way as podoplanin-transfected CHO/hPDPN. Furthermore, NZ-8 reacted
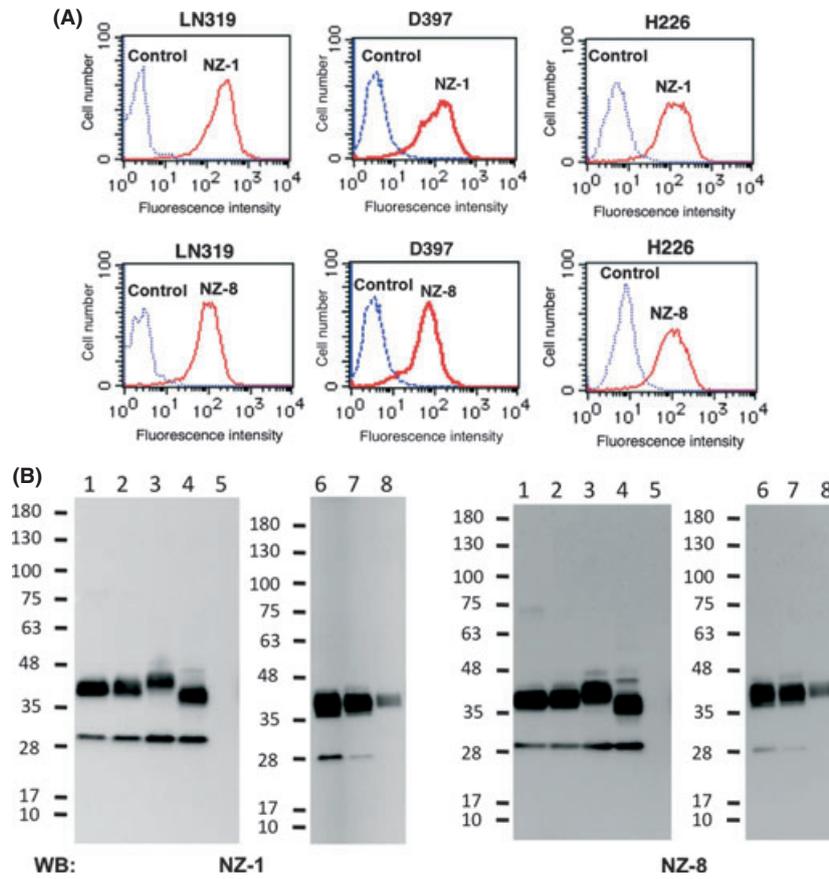
Fig. 1. Characterization of chimeric anti-podoplanin antibody, NZ-8. (A) LN319 and D397 human glioblastoma cells and H226 human malignant mesothelioma cells were treated with NZ-1 or NZ-8 (1 μg/mL). (B) The membrane was incubated with NZ-1 or NZ-8 (1 μg/mL). Lane 1, CHO cells transfected with human podoplanin (CHO/hPDPN); lane 2, Lec1/hPDPN; lane 3, Lec2/hPDPN; lane 4, Lec8/hPDPN; lane 5, CHO; lane 6, LN319; lane 7, lymphatic endothelial cells; lane 8, H226. WB, Western blot.
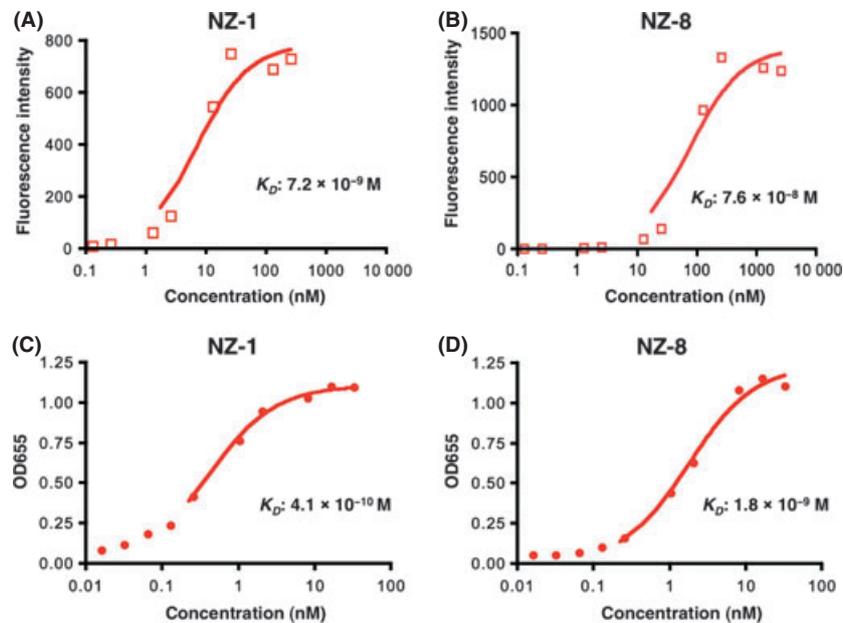

Fig. 2. Determination of binding-affinity using flow cytometry and ELISA. LN319 human glioblastoma cells (2×10^5) were resuspended at 100 μL serially diluted NZ-1 (A) or NZ-8 (B) (0.01–20 μg/mL). The plates were incubated with serially diluted NZ-1 (C) or NZ-8 (D) (150 pg/mL–2.5 μg/mL). K_D, dissociation constant.
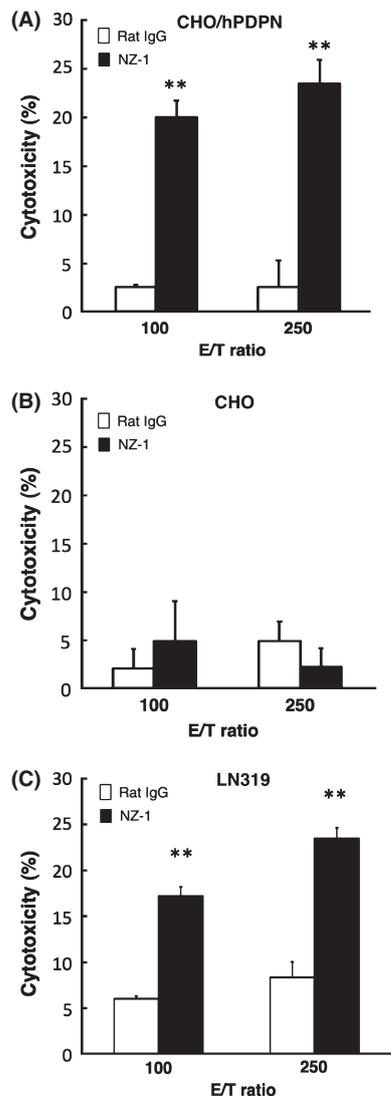
Fig. 3. Antibody-dependent cellular cytotoxicity activities induced by rat splenocytes against CHO cells transfected with human podoplanin (CHO/hPDPN) (A), CHO (B), and glioblastoma cell line LN319 (C), were determined with 6-h ^{51}Cr release assays at the effector/target (E/T) ratio of 100 and 250 in the presence of 1 μg/mL of NZ-1. **P < 0.01 versus control (values are means ± SE).
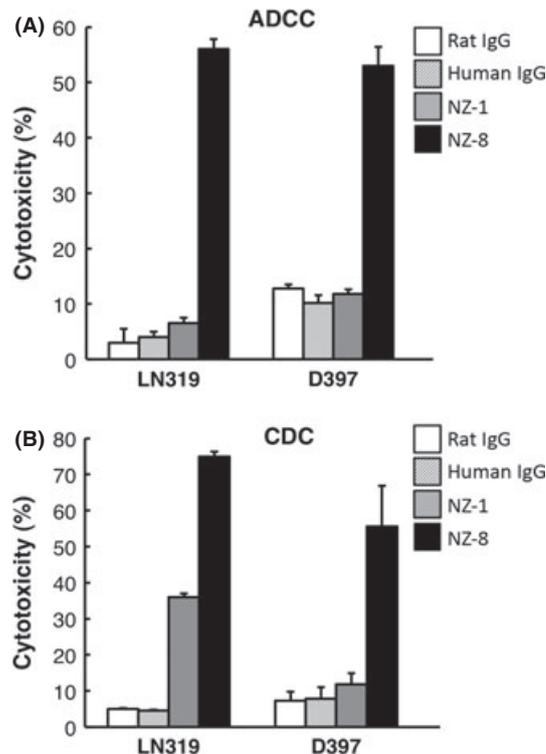

Fig. 4. Antibody-dependent cellular cytotoxicity (ADCC) and complement-dependent cytotoxicity (CDC) activities of anti-podoplanin antibodies. (A) ADCC activities induced by human mononuclear cells against glioblastoma cell lines LN319 and D397 were determined with 6-h ^{51}Cr release assay at the effector/target ratio of 100 in the presence of 1 μg/mL NZ-1, NZ-8, rat IgG, and human IgG. (B) CDC activities against glioblastoma cell lines LN319 and D397 were shown by ^{51}Cr release assay. **P < 0.01 versus control (values are means ± SE).

with glioblastoma cell line LN319, mesothelioma cell line H226, and human lymphatic endothelial cells. Because the binding-affinity of antibodies is critical for antibody-based cancer therapy, dissociation constant (K_D) was next determined using flow cytometric analysis or ELISA.[28] As shown in Figure 2(A,C), K_D of NZ-1 was determined to be 7.2×10^{-9} M by flow cytometry or 4.1×10^{-10} M by ELISA. Using the same methods, K_D of NZ-8 was determined to be 7.6×10^{-8} M by flow cytometry or 1.8×10^{-9} M by ELISA (Fig. 2B,D).

Antibody-dependent cellular cytotoxicity (ADCC) and complement-dependent cytotoxicity (CDC) mediated by anti-podoplanin antibodies. To apply targeted therapy to podoplanin, we further assessed whether anti-podoplanin antibodies can induce ADCC against podoplanin-expressing cell lines mediated by rat splenocytes or human MNC as effector cells. Antibody-dependent cellular cytotoxicity by NZ-1 was observed against CHO/hPDPN cells, when rat splenocytes were used as effector cells (Fig. 3A), whereas it was not observed against CHO cells

(Fig. 3B). Antibody-dependent cellular cytotoxicity by NZ-1 was also observed against LN319 glioblastoma cells (Fig. 3C). We next compared the ADCC and CDC activities between NZ-1 and NZ-8 using LN319 and D397. Antibody-dependent cellular cytotoxicity against glioblastoma cell lines was not shown by NZ-1 using human MNC, whereas NZ-8 showed the induction of significant levels of ADCC mediated by human MNCs against LN319 and D397 glioblastoma cells (Fig. 4A). Furthermore, CDC was induced by NZ-8 against LN319 and D397, which was significantly higher than that of NZ-1 (Fig. 4B).

Antitumor activity of anti-podoplanin antibodies on the growth of podoplanin-expressing cells _in vivo._ We first investigated the antitumor activity of NZ-1 _in vivo_ (Fig. 5). The subcutaneous tumor formation rate was 9/10 (90%) for the control group and 6/9 (66.6%) for the group given NZ-1 antibody. Subcutaneous tumors were significantly smaller in the group given NZ-1 antibody after 50 days of cell implantation, as compared with the control group (Fig. 5A), indicating that inoculation with NZ-1 significantly inhibited the growth of CHO/hPDPN cells _in vivo_. Spontaneous metastasis of CHO/hPDPN was also observed; the lung nodules of CHO/hPDPN of NZ-1 groups were less than those of rat IgG groups (Fig. 5B, P < 0.05). Staining with H&E revealed that several metastatic foci were detected in control lungs, whereas much fewer metastatic foci were observed in lung NZ-1 groups (Fig. 5C). We next investigated the antitumor activity of NZ-8 _in vivo_. Tumor formation incidence was 10/10 (100%) for the control group and 4/10 (40%) for the NZ-8 group. Subcutaneous
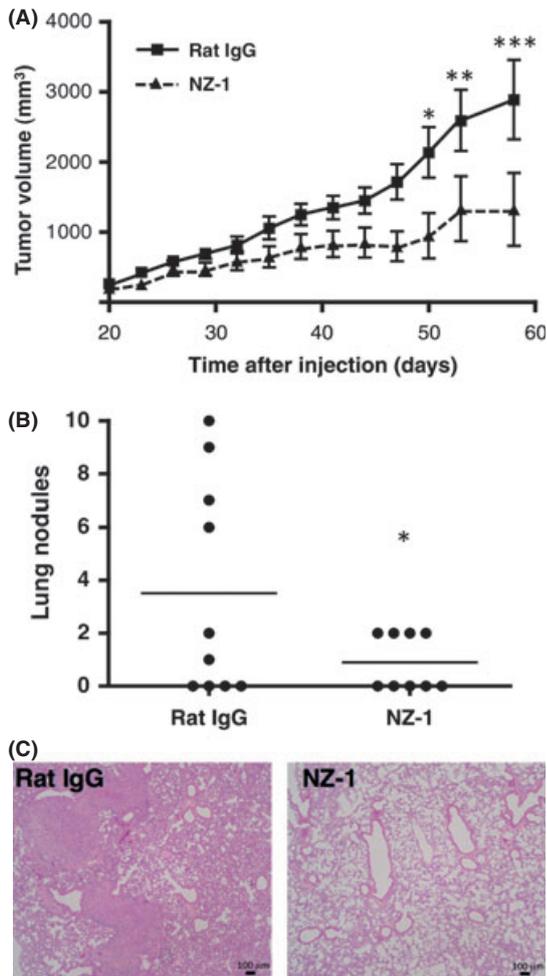
Fig. 5. Antitumor activity of NZ-1 on the growth of podoplanin-expressing cells *in vivo*. (A) CHO cells transfected with human podoplanin (CHO/hPDPN; 3.0×10^7 cells/mL) were s.c. implanted into BALB/c nude mice at a dose of 100 μL/animal. After 1 day, NZ-1 (5 mg/mL) or rat IgG (5 mg/mL) was given at 0.5 μL/h for 2 weeks sustainably (control group, $n = 10$; NZ-1 group, $n = 9$). Twenty days after cell implantation, tumor diameter was measured at intervals of 3 days. *$P < 0.05$; **$P < 0.01$; ***$P < 0.001$ by two-way ANOVA. (B,C) Spontaneous metastasis of CHO/hPDPN was observed. (B) number of lung metastatic foci. *$P < 0.05$ by *t*-test. (C) H&E staining.

Fig. 6. Antitumor activity of NZ-8 on the growth of podoplanin-expressing cells *in vivo*. (A) Podoplanin-expressing CHO cells transfected with human podoplanin (CHO/hPDPN; 3.0×10^6 cells) were s.c. implanted into BALB/c nude mice. NZ-8 or normal human IgG (100 μg/mouse) was given every week ($n = 10$/group). (B) Comparison of tumor size (day 40).*$P < 0.05$; **$P < 0.01$; ***$P < 0.001$ by two-way ANOVA.

tumors were significantly smaller in the group given NZ-8 antibody compared to the control group (Fig. 6), indicating that inoculation with NZ-8 also significantly inhibited the growth of CHO/hPDPN cells *in vivo*.

Suppression of tumor metastasis by anti-podoplanin antibodies. We then investigated the inhibitory effect of anti-podoplanin antibodies against podoplanin-induced platelet aggregation. We previously clarified that NZ-1 recognizes the platelet aggregation-stimulating domain, and neutralizes podoplanin-induced platelet aggregation. Results showed that NZ-8 inhibited platelet aggregation by CHO/hPDPN in a dose-dependent manner (Fig. 7A), although NZ-1 inhibited CHO/hPDPN-induced platelet aggregation more effectively than NZ-8 at a dose of 1 mg/mL.

We next investigated whether anti-podoplanin antibodies could suppress the podoplanin-induced pulmonary metastasis in an experimental metastasis model. Injection of CHO/hPDPN cells led to development of multiple lung metastatic foci. The number of metastatic lung nodules in mice injected with CHO/
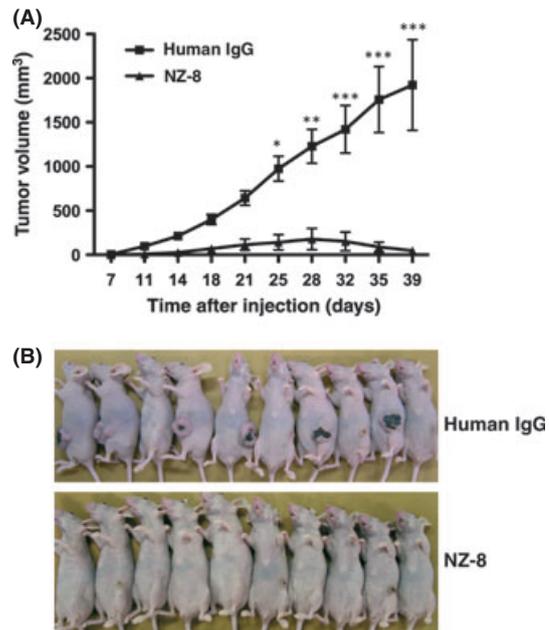
hPDPN + NZ-1 was significantly lower than that in CHO/hPDPN + control PBS (Fig. 7B, $P < 0.05$). We did not observe, macroscopically, metastatic foci in the liver, kidney, spleen, colon, or ovary in any of the mice (data not shown). Furthermore, we investigated whether NZ-8 could also suppress podoplanin-induced pulmonary metastasis in the same model. As shown in Figure 7(B), NZ-8 also suppressed pulmonary metastasis. The number of metastatic lung nodules in mice injected with CHO/hPDPN + NZ-8 was significantly lower than that in CHO/hPDPN + control PBS in the same way with NZ-1 (Fig. 7B, $P < 0.05$). Staining with H&E revealed that many metastatic foci were detected in control lung, whereas much fewer metastatic foci were observed in lung in NZ-1 and NZ-8 groups (Fig. 7C). Furthermore, dose-dependency of the antimetastatic effects by NZ-8 was examined. As shown in Figure 7(D,E), CHO/hPDPN-induced lung metastasis was reduced significantly by both 10 μg ($P < 0.05$) and 50 μg ($P < 0.001$) NZ-8 in a dose-dependent manner. These results indicate that both NZ-1 and NZ-8 inhibited significantly pulmonary metastasis as compared to control, suggesting that anti-podoplanin antibodies may be effective in podoplanin-induced tumor metastasis.

Discussion

In this study, we produced a human–rat chimeric anti-podoplanin mAb, NZ-8, which showed high reactivity with podoplanin-expressing cell lines in flow cytometry and Western blot analyses (Fig. 1). Although NZ-8 possesses lower affinity compared with NZ-1 (Fig. 2), NZ-8 showed the induction of significant levels of ADCC and CDC against glioblastoma cells compared with NZ-1 (Fig. 4), indicating that targeting podoplanin-expressing tumors with NZ-8 seems to be useful for antibody-based immunotherapy. Generally, the CDC activity of antibody is known to be dependent on the IgG subclass;
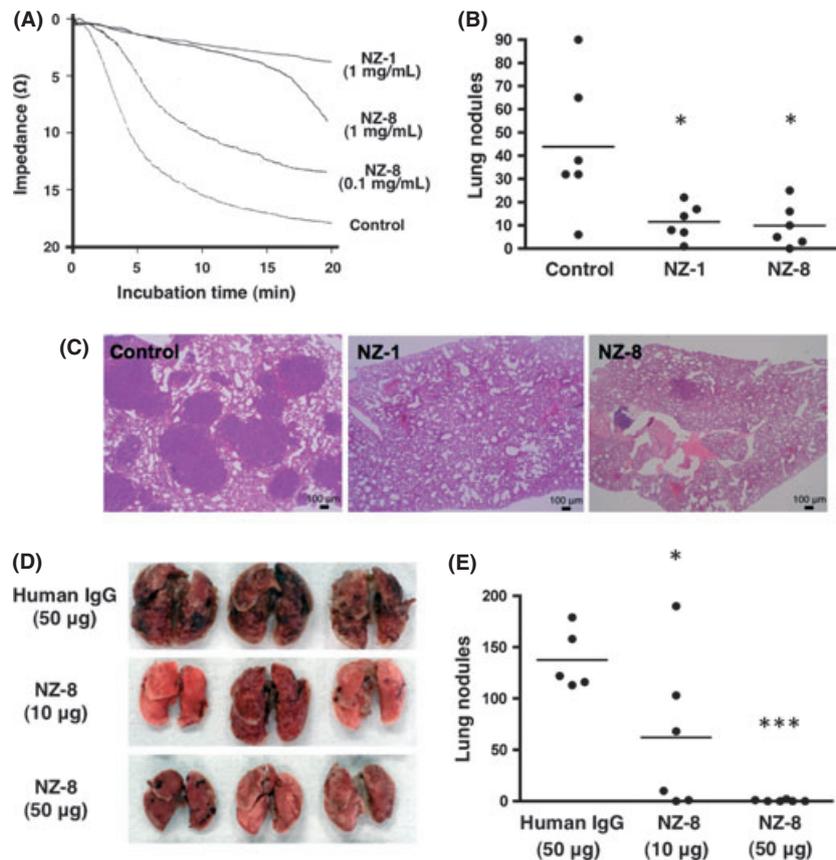
Fig. 7. Suppression of tumor metastasis by anti-podoplanin antibodies. (A) Platelet aggregation was initiated by the addition of CHO cells transfected with human podoplanin (CHO/hPDPN; 5×10^6) and monitored for 20 min. (B,C) CHO/hPDPN cells (5×10^6 cells/mL) were incubated with 100 μg NZ-1 or NZ-8, and inoculated i.v. (5×10^5 cells/mouse) into BALB/c-nu/nu mice. (B) Number of lung metastatic foci. *$P < 0.05$ by ANOVA with Tukey–Kramer multiple comparisons. (C) H&E staining. (D,E) CHO/hPDPN cells (5×10^6 cells/mL) were incubated with 50 μg human IgG, 10 μg NZ-8, or 50 μg NZ-8, and inoculated i.v. (5×10^5 cells/mouse) into BALB/c-nu/nu mice. (D) Lung metastatic foci. (E) Number of lung metastatic foci. *$P < 0.05$; ***$P < 0.001$ by ANOVA with Tukey–Kramer multiple comparisons.

human IgG_1 and IgG_3 possess higher CDC activity, and rat IgG_{2b} subclass has higher CDC activity compared with other subclasses. Therefore, NZ-8 of human IgG_1 might show much higher CDC activity compared with NZ-1 of rat IgG_{2a}.

It has been shown that NZ-1 suppresses podoplanin-induced pulmonary metastasis through inhibiting platelet aggregation.[12] In this study, NZ-1 also inhibited platelet aggregation using another whole blood aggregometer system (Fig. 7A). NZ-8 inhibited platelet aggregation in a dose-dependent manner; however, the inhibition seems to be weaker than that of NZ-1, probably because of the low binding-affinity against podoplanin-expressing cells. To date, the suppression of tumor metastasis by podoplanin has been reported to be dependent on platelet aggregation, because not only whole IgGs of NZ-1 but also $F(ab')_2$ fragments of NZ-1 almost completely suppressed pulmonary metastasis of CHO/hPDPN cells.[12] However, other effector functions, such as ADCC and CDC, of NZ-1 remain to be investigated. In the present study, NZ-1 and NZ-8 clearly showed ADCC and CDC activities (Figs 3,4). NZ-1 and NZ-8 also inhibited the growth of CHO/hPDPN cells *in vivo* (Figs 5,6). Although the neutralizing activity of NZ-8 seems to be weaker than that of NZ-1 (Fig. 7A), effective suppression of pulmonary metastasis by NZ-8 was observed at the same level as NZ-1 (Fig. 7B–E), indicating that suppression of pulmonary metastasis may be dependent on both neutralizing activity and ADCC/CDC activities. We carried out additional experiments of ^{51}Cr release assay to show that NZ-1 and NZ-8 possess ADCC activities against tumor cells, using mouse splenocytes. However, neither NZ-1 nor NZ-8 could clearly induce ADCC activity using mouse splenocytes (data not shown). In contrast, both NZ-1 and NZ-8 showed high CDC activities (Fig. 4B); therefore, we speculate that the antitumor effects of NZ-1 and NZ-8 against tumor cells *in vivo* may be induced mainly by their CDC activity, especially in a mouse model. Importantly, podoplanin has been reported to be expressed in lymphatic endothelial cells, podocytes, and type I alveolar cells, suggesting that there are possibilities to induce side-effects for human cancer treatment using NZ-8. Therefore, the toxicity test should be carried out using monkeys in the near future.[32] We have shown that podoplanin expression in normal tissue is much lower than that of tumors;[1] therefore, the side-effects of anti-podoplanin antibodies could be reduced by decreasing the dosage of NZ-8 antibody.

In conclusion, we clarified that anti-podoplanin antibodies possess potent and therapeutic antitumor effects based on ADCC and CDC against podoplanin-expressing cells. These results suggest that targeting therapy to podoplanin with therapeutic antibodies might be useful as a novel immunotherapy against podoplanin-expressing tumors such as malignant brain tumors, mesotheliomas, and squamous cell carcinoma.

Disclosure Statement

The authors have no conflicts of interest.

References

1 Kato Y, Fujita N, Kunita A *et al.* Molecular identification of Aggrus/T1alpha as a platelet aggregation-inducing factor expressed in colorectal tumors. *J Biol Chem* 2003; **278**: 51599–605.

2 Breiteneder-Geleff S, Soleiman A, Kowalski H *et al.* Angiosarcomas express mixed endothelial phenotypes of blood and lymphatic capillaries: podoplanin as a specific marker for lymphatic endothelium. *Am J Pathol* 1999; **154**: 385–94.

3 Kato Y, Sasagawa I, Kaneko M, Osawa M, Fujita N, Tsuruo T. Aggrus: a diagnostic marker that distinguishes seminoma from embryonal carcinoma in testicular germ cell tumors. *Oncogene* 2004; **23**: 8552–6.

4 Kato Y, Kaneko M, Sata M, Fujita N, Tsuruo T, Osawa M. Enhanced expression of Aggrus (T1alpha/podoplanin), a platelet-aggregation-inducing factor in lung squamous cell carcinoma. *Tumor Biol* 2005; **26**: 195–200.

5 Kato Y, Kaneko MK, Kuno A *et al.* Inhibition of tumor cell-induced platelet aggregation using a novel anti-podoplanin antibody reacting with its platelet-aggregation-stimulating domain. *Biochem Biophys Res Commun* 2006; **349**: 1301–7.

6 Kimura N, Kimura I. Podoplanin as a marker for mesothelioma. *Pathol Int* 2005; **55**: 83–6.

7 Mishima K, Kato Y, Kaneko MK *et al.* Podoplanin expression in primary central nervous system germ cell tumors: a useful histological marker for the diagnosis of germinoma. *Acta Neuropathol (Berl)* 2006; **111**: 563–8.

8 Mishima K, Kato Y, Kaneko MK, Nishikawa R, Hirose T, Matsutani M. Increased expression of podoplanin in malignant astrocytic tumors as a novel molecular marker of malignant progression. *Acta Neuropathol (Berl)* 2006; **111**: 483–8.

9 Kunita A, Kashima TG, Ohazama A, Grigoriadis AE, Fukayama M. Podoplanin is regulated by AP-1 and promotes platelet aggregation and cell migration in osteosarcoma. *Am J Pathol* 2011; **179**: 1041–9.

10 Gandarillas A, Scholl FG, Benito N, Gamallo C, Quintanilla M. Induction of PA2.26, a cell-surface antigen expressed by active fibroblasts, in mouse epidermal keratinocytes during carcinogenesis. *Mol Carcinog* 1997; **20**: 10–8.

11 Sugimoto Y, Watanabe M, Oh-hara T, Sato S, Isoe T, Tsuruo T. Suppression of experimental lung colonization of a metastatic variant of murine colon adenocarcinoma 26 by a monoclonal antibody 8F11 inhibiting tumor cell-induced platelet aggregation. *Cancer Res* 1991; **51**: 921–5.

12 Kato Y, Kaneko MK, Kunita A *et al.* Molecular analysis of the pathophysiological binding of the platelet aggregation-inducing factor podoplanin to the C-type lectin-like receptor CLEC-2. *Cancer Sci* 2008; **99**: 54–61.

13 Kunita A, Kashima TG, Morishita Y *et al.* The platelet aggregation-inducing factor aggrus/podoplanin promotes pulmonary metastasis. *Am J Pathol* 2007; **170**: 1337–47.

14 Martin-Villar E, Megias D, Castel S, Yurrita MM, Vilaro S, Quintanilla M. Podoplanin binds ERM proteins to activate RhoA and promote epithelial-mesenchymal transition. *J Cell Sci* 2006; **119**: 4541–53.

15 Hoshino A, Ishii G, Ito T *et al.* Podoplanin-positive fibroblasts enhance lung adenocarcinoma tumor formation: podoplanin in fibroblast functions for tumor progression. *Cancer Res* 2011; **71**: 4769–79.

16 Kono T, Shimoda M, Takahashi M *et al.* Immunohistochemical detection of the lymphatic marker podoplanin in diverse types of human cancer cells using a novel antibody. *Int J Oncol* 2007; **31**: 501–8.

17 Roy S, Chu A, Trojanowski JQ, Zhang PJ. D2-40, a novel monoclonal antibody against the M2A antigen as a marker to distinguish hemangioblastomas from renal cell carcinomas. *Acta Neuropathol (Berl)* 2005; **109**: 497–502.

18 Scholl FG, Gamallo C, Quintanilla M. Ectopic expression of PA2.26 antigen in epidermal keratinocytes leads to destabilization of adherens junctions and malignant progression. *Lab Invest* 2000; **80**: 1749–59.

19 Yuan P, Temam S, El-Naggar A *et al.* Overexpression of podoplanin in oral cancer and its association with poor clinical outcome. *Cancer* 2006; **107**: 563–9.

20 Kawaguchi H, El-Naggar AK, Papadimitrakopoulou V *et al.* Podoplanin: a novel marker for oral cancer risk in patients with oral premalignancy. *J Clin Oncol* 2008; **26**: 354–60.

21 Kawase A, Ishii G, Nagai K *et al.* Podoplanin expression by cancer associated fibroblasts predicts poor prognosis of lung adenocarcinoma. *Int J Cancer* 2008; **123**: 1053–9.

22 Hatakeyama K, Kaneko MK, Kato Y *et al.* Podoplanin expression in advanced atherosclerotic lesions of human aortas. *Thromb Res* 2012; **129**: 70–6.

23 Singh SK, Hawkins C, Clarke ID *et al.* Identification of human brain tumour initiating cells. *Nature* 2004; **432**: 396–401.

24 Bao S, Wu Q, McLendon RE *et al.* Glioma stem cells promote radioresistance by preferential activation of the DNA damage response. *Nature* 2006; **444**: 756–60.

25 Atsumi N, Ishii G, Kojima M, Sanada M, Fujii S, Ochiai A. Podoplanin, a novel marker of tumor-initiating cells in human squamous cell carcinoma A431. *Biochem Biophys Res Commun* 2008; **373**: 36–41.

26 Kato Y, Vaidyanathan G, Kaneko MK *et al.* Evaluation of anti-podoplanin rat monoclonal antibody NZ-1 for targeting malignant gliomas. *Nucl Med Biol* 2010; **37**: 785–94.

27 Kaneko M, Kato Y, Kunita A, Fujita N, Tsuruo T, Osawa M. Functional sialylated O-glycan to platelet aggregation on Aggrus (T1alpha/podoplanin) molecules expressed in Chinese Hamster Ovary cells. *J Biol Chem* 2004; **279**: 38838–43.

28 Stein RA, Wilkinson JC, Guyer CA, Staros JV. An analytical approach to the measurement of equilibrium binding constants: application to EGF binding to EGF receptors in intact cells measured by flow cytometry. *Biochemistry* 2001; **40**: 6142–54.

29 Kaneko MK, Tian W, Takano S *et al.* Establishment of a novel monoclonal antibody SMab-1 specific for IDH1-R132S mutation. *Biochem Biophys Res Commun* 2011; **406**: 608–13.

30 Wang W, Nishioka Y, Ozaki S *et al.* HM1.24 (CD317) is a novel target against lung cancer for immunotherapy using anti-HM1.24 antibody. *Cancer Immunol Immunother* 2009; **58**: 967–76.

31 Kishuku M, Nishioka Y, Abe S *et al.* Expression of soluble vascular endothelial growth factor receptor-1 in human monocyte-derived mature dendritic cells contributes to their antiangiogenic property. *J Immunol* 2009; **183**: 8176–85.

32 Kaji C, Tsujimoto Y, Kaneko MK, Kato Y, Sawa Y. Immunohistochemical examination of novel rat monoclonal antibodies against mouse and human podoplanin. *Acta Histochem Cytochem* (in press).